

## Microwave Absorption Properties of Co, Cu, Zn - Substituted Hexaferrite Polychloroprene Nanocomposites

Valeska da Rocha Caffarena<sup>a\*</sup>, Jefferson Leixas Capitaneio<sup>b</sup>,

Tsuneharu Ogasawara<sup>c</sup>, Magali Silveira Pinho<sup>d</sup>

<sup>a</sup>PETROBRAS – Gás & Energia - Corporativo,  
Tecnologia para Processos de Gás e Energia, Tecnologia para Processos de Gás Natural

<sup>b</sup>Instituto de Macromoléculas – IMA,

Universidade Federal do Rio de Janeiro – UFRJ

<sup>c</sup>Programa de Eng. Metalúrgica e de Materiais, COPPE,

Universidade Federal do Rio de Janeiro – UFRJ

<sup>d</sup>Instituto de Pesquisas da Marinha – IPqM

Received: December 10, 2007; Revised: February 27, 2008

The magnetic behavior and its relationship with microwave absorbing properties have been investigated for doped Z-type barium hexaferrites ( $\text{Ba}_3\text{Co}_{1.3}\text{Zn}_{0.3}\text{Cu}_{0.4}\text{Fe}_{24}\text{O}_{41}$ ) polychloroprene (CR) nanocomposites.

Simultaneous substitutions by  $\text{Co}^{2+}$ ,  $\text{Cu}^{2+}$ , and  $\text{Zn}^{2+}$  ions make possible the use of these materials as RAMs, due to the frequency dependence of  $\mu_r^*$  (permeability), responsible for the location of the hexaferrite natural resonance.

The  $\text{Cu}^{2+}$  ions distort the crystalline field due to their electronic configuration, and this behavior results in an increase in the saturation magnetization ( $M_s$ ), which improve the magnetic permeability. Similarly, the superparamagnetic contribution (associated to the nanometric size) led to the improvement of the microwave absorption.

**Keywords:** Z-type hexaferrite, radar absorption material, permittivity, permeability, magnetic properties

### 1. Introduction

The term “nanocomposite” refers to a composite at least one dimension is in the nanometer range. The definition of nanocomposite material has broadened significantly to encompass a large variety of systems such as one-dimensional, two-dimensional, three-dimensional and amorphous materials, made of distinctly dissimilar components and mixed at the nanometer scale<sup>1</sup>.

The properties of nanocomposite materials depend not only on the properties of their individual parents but also on their morphology and interfacial characteristics.

Nanoscale magnetic systems display a large variety of interesting physical properties, forming a unique group for the study of diverse problems in solid state physics, such as superparamagnetism<sup>1-3</sup>.

In this work, the effect of temperature variation on the magnetization curves was measured for  $\text{Ba}_3\text{Co}_{1.3}\text{Zn}_{0.3}\text{Cu}_{0.4}\text{Fe}_{24}\text{O}_{41}$  hexaferrite nanometric powder synthesized by the citrate precursor method, to evaluate the superparamagnetic (SPM) contribution to the microwave absorption properties<sup>1</sup>. Thus, the magnetic properties and its relationship with microwave absorbing properties have been investigated.

As is well known<sup>1-3</sup>, the decrease of particle size within the range of single-domain and nanometric dimensions is accompanied by drops in the remanence and the coercivity, which becomes null in a critical size, below which the particle is called superparamagnetic (SPM)<sup>1</sup>.

The shape of the hysteresis curve for SPM particle powders is extremely fine and its behavior is very similar to that of paramagnetic materials, but the grains present high magnetic moments.

In single-domain particles (SD) smaller than a given value<sup>1</sup> the coercivity decreases with the reduction in particle size due to the ef-

fects of thermal energy randomization. As the particle size decreases within the multi-domain (MD) range, the coercivity decreases up to a maximum in a critical particle size where it is no longer possible to accommodate a domain wall and the particle can only exist as a single-domain<sup>1-3</sup>.

The change in the magnetization of MD particles requires the translation of the domain walls, a process that is energetically easy and is observed in a relatively small magnetic field<sup>1</sup>. The SD particles can only be magnetized by rotation of the magnetization, an energetically difficult process.

The synthesized Z-type barium hexaferrite was mixed with polychloroprene (CR) in order to obtain samples for the microwave absorption measurements, resulting in the 80:20 (wt. (%), ferrite:polychloroprene) nanocomposite.

When the ferrite particle size is nanometric, the superparamagnetic contribution due to small particles (above 10 nm diameter) may lead to a great improve in the absorbing properties<sup>1</sup>. If the particle size of an absorber is small enough and the discrete energy level spacing is in the energy range of microwaves, the electron can absorb the energy as it leaps from one level to another, which may lead to the increment of the microwave absorption<sup>1-2</sup>.

### 2. Materials and Methods

Nanosized  $(\text{Zn-Co-Cu})_2\text{-Z}$  type powders (10-300 nm) were synthesized by the citrate precursor method (Figure 1), using the following reagents:  $\text{Fe}(\text{NO}_3)_3 \cdot 9\text{H}_2\text{O}$ ,  $\text{Ba}(\text{NO}_3)_2$ , monohydrate citric acid,  $\text{Co}(\text{NO}_3)_2 \cdot 6\text{H}_2\text{O}$ ,  $\text{Cu}(\text{NO}_3)_2 \cdot 3\text{H}_2\text{O}$  and  $\text{Zn}(\text{NO}_3)_2 \cdot 6\text{H}_2\text{O}$ , in

\*e-mail: valeskac@petrobras.com.br

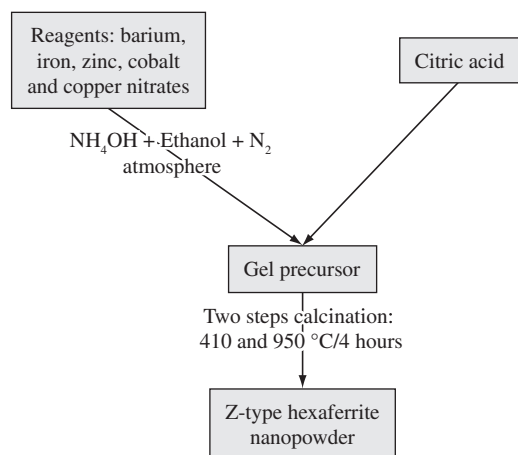


**Figure 1.** Diagram of the  $\text{Ba}_3\text{Co}_{1.3}\text{Zn}_{0.3}\text{Cu}_{0.4}\text{Fe}_{24}\text{O}_{41}$  hexaferrite preparation by the citrate precursor method.

stoichiometric molar ratios to achieve the  $\text{Ba}_3\text{Co}_{1.3}\text{Zn}_{0.3}\text{Cu}_{0.4}\text{Fe}_{24}\text{O}_{41}$  hexaferrite. The preparation of the solutions was carried out by weighting the reagents and placing them into adequate vessels. Bidistilled water was added to each one, under agitation, until total dissolution of the solids.

Then, the solutions were transferred to a round bottom flask (2,000 mL) and mixed. The resulting mixture was heated under reflux up to 70 °C to complete the reaction, in order to allow the addition of  $\text{NH}_4\text{OH}$ , drop by drop into the solution to make it neutral or slightly alkaline, for subsequent precipitation of the organo-metallic complex<sup>4</sup>.

The key metal cations reacted with citric acid, under controlled pH conditions, to give the respective metal citrate, making up a homogeneous joint metallic citrate precursor complex.

Ethanol was then added under vigorous stirring, into the reacting mixture to promote the precipitation of a complex citrate gel of barium, iron, zinc, copper and cobalt. After that, the remaining aqueous solution was removed by drying it at 70 °C. The remaining desired solid phase was a highly viscous residue. All the synthesis process was carried out in a  $\text{N}_2$  inert atmosphere.

Similarly, the ultrafine  $\text{Co}_2\text{Z}$  powders were also synthesized by using citrate precursor method, from  $\text{Fe}(\text{NO}_3)_3 \cdot 9\text{H}_2\text{O}$ ,  $\text{Ba}(\text{NO}_3)_2$ , monohydrate citric acid and  $\text{Co}(\text{NO}_3)_2 \cdot 6\text{H}_2\text{O}$  stoichiometric molar ratios to achieve  $\text{Ba}_3\text{Co}_2\text{Fe}_{24}\text{O}_{41}$ . The  $\text{Ba}_3\text{Co}_2\text{Fe}_{24}\text{O}_{41}$  ferrite was used to compare its magnetic properties with  $\text{Ba}_3\text{Co}_{1.3}\text{Zn}_{0.3}\text{Cu}_{0.4}\text{Fe}_{24}\text{O}_{41}$  hexaferrite.

The determination of the ideal temperature for the citrate gel decomposition, as well as the whole behavior of the mixture under heating, was carried out by using thermogravimetric and differential thermal analysis. Based on the results from the thermal analyses, the gel was submitted to a calcination performed according to the following heating schedule: 2 °C/min up to 410 °C, a 410 °C plateau for 1 hour, 10 °C/minute up to the final calcination temperature from 600 to 1,200 °C (with a residence time at the calcination temperature of 4 hours). Then, it was cooled down at 10 °C/min to room temperature.

The calcined products (from 600 to 1,200 °C) were submitted to X ray diffraction in order to assure the formation of the magnetic crystalline phase of the Z-type barium hexaferrite<sup>5</sup> ( $\text{Ba}_3\text{Co}_{1.3}\text{Zn}_{0.3}\text{Cu}_{0.4}\text{Fe}_{24}\text{O}_{41}$ ), which only occurs at 950 °C.

Unlike preparation of pure  $\text{BaFe}_{12}\text{O}_{19}$  (M-type hexaferrite) by citrate precursor method, the Z-type phase powder can not be produced so easily due to the complexity of its structure, which imposes

progressive transformation through intermediate ferrites before an achieving the final required structure<sup>5</sup>.

For this analysis, the solid materials were placed on a glass sample holder and spread out to form a thin layer. A Siemens AXS D5005 diffractometer in the  $\theta$ -2 $\theta$  Bragg-Brentano geometry with a dwell time of 1 °/minute was employed.

Thermogravimetry (TG) and Differential Thermal Analyses (DTA) were carried out by using a TA Instruments SDT-2960. The experiments were carried out in static air, using platinum crucibles between 20 and 1,000 °C, with a heating rate of 10 °C/minute.

X ray fluorescence measurements were carried out in a Philips model PW 2400 sequential spectrometer. This quantitative method was used to determine the stoichiometry of the ferrite samples, which were analyzed in the form of fused beads, using lithium tetraborate flux.

The morphological study was performed using a Topometrix II® Atomic Force Microscopy (AFM) and a Zeiss Scanning Electron Microscope (SEM) model DSM 940 A, operating at acceleration voltages of 20 kV, 24 kV and 25 kV.

The magnetic hysteresis loops of  $\text{Ba}_3\text{Co}_2\text{Fe}_{24}\text{O}_{41}$  and  $\text{Ba}_3\text{Co}_{1.3}\text{Zn}_{0.3}\text{Cu}_{0.4}\text{Fe}_{24}\text{O}_{41}$  compositions were obtained by using the vibrating sample magnetometer (VSM) 4,500 PAR. The effect of the temperature variation on the magnetization curves of  $\text{Ba}_3\text{Co}_{1.3}\text{Zn}_{0.3}\text{Cu}_{0.4}\text{Fe}_{24}\text{O}_{41}$  hexaferrite nanopowder was determined by using the Physical Property Measurement System (PPMS) extraction magnetometer Model 6,000, in a temperature lower than the melting temperature of helium (4.2 K).

The composite specimens for measuring microwave absorber properties were prepared by mixing, molding and curing mixtures of barium hexaferrite powders with polychloroprene (CR, neoprene W of Du Pont, density 1.21 g.cm<sup>-3</sup>) and the additives of vulcanization. This resulted in a barium hexaferrite:polychloroprene concentration of 80:20 by weight.

The processing was carried out in a Berstorff mill at room temperature, with velocities of 22 and 25 rpm (back and forward). Vulcanized samples with 8.00 × 4.00 × 0.10 cm<sup>3</sup> in size were obtained by compression molding in an hydraulic press at 150 °C and 6.7 MPa. The curing times were determined from the data obtained with a Monsanto Rheometer TM100. The dispersion of the magnetic particles in CR was evaluated by using Scanning Electron Microscopy (SEM).

The microwave measurements were based on the transmission/reflection method (T/R) using a rectangular waveguide as the confining medium for the samples<sup>6-10</sup>. A network analyzer was used to measure the magnitude and phase response of the samples under test (SUT) by the comparison with the signal transmitted by the SUT and that reflected from its input. The measurements were made with a HP 8510 network analyzer system which consists of a HP 8510B network analyzer, a HP 83622 A synthesized sweeper and a HP 8515 A S-parameter test-set<sup>9,10</sup>. The material was analyzed in the frequency ranges from 2.6 to 4.0 GHz (S-band) and 8.0 to 16.0 GHz (X/Ku- bands).

From the data obtained, a prediction of the microwave reflectivity levels for the sheet absorbers with other thickness values (2.0-6.0 mm) was made to estimate the variations of reflection loss (dB) vs. frequency (GHz).

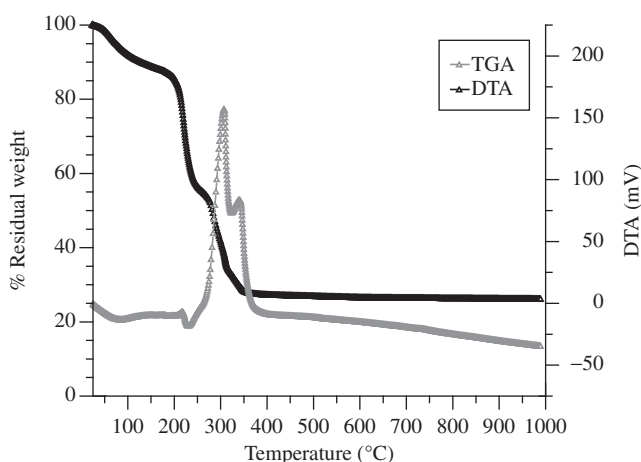
### 3. Results and Discussion

Results from the X ray fluorescence analysis (XRF) confirmed that the synthesized powders achieved the planned stoichiometry (Table 1).

The DTA/TG results for the citrate dried gels prepared are shown in Figure 2.

**Table 1.** Stoichiometry composition for  $\text{Ba}_3\text{Co}_{1.3}\text{Zn}_{0.3}\text{Cu}_{0.4}\text{Fe}_{24}\text{O}_{41}$  obtained by XRF analysis.

Chemical compound	Weight (%)	
	Theoretic	Experimental
Ba	16.2849	16.28
Co	3.0283	3.03
Zn	0.7754	0.78
Cu	1.0047	1.00
Fe	52.9781	52.98
BaO	18.1821	18.18
CoO	3.8504	3.85
ZnO	0.9652	0.97
CuO	1.2577	1.28
$\text{Fe}_2\text{O}_3$	75.7446	75.75

**Figure 2.** TG-DTA curves for the precursor gel.

The endothermic peak around 100 °C in the DTA curve with a small weight loss (~2%), is due to the loss of residual water in the gel. The first sharp exothermic peak at about 217 °C with a concurrent large weight loss of ~60% could be due to the reaction of metal cations (Ba, Co, Cu, Zn, Fe) with citric acid<sup>4</sup>.

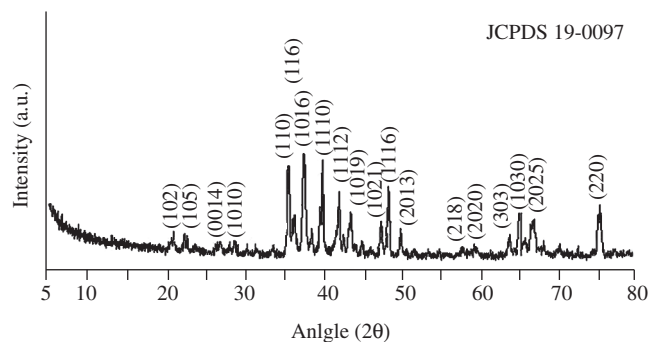
Whereas, the decomposition of unreacted starting citric acid remained after combustion could be responsible for the exothermic peak at about 360 °C.

From the results, it was observed that there was no significant loss of weight over 410 °C. Therefore, the gel was heated to this temperature with rate of 2 °C/min, and the temperature was kept there for 60 minutes to ensure the complete elimination of the organic precursor during the calcination process.

To determine the lowest temperature for the formation of the phase of Z-type barium hexaferrite, the powder was calcined in a second step above 600 °C and crystalline phases present were determined by X ray diffraction.

X ray Diffraction analysis indicates that at 950 °C, the Z-type phase was clearly the majority one (Figure 3). However, according to the literature<sup>11</sup> this material could contains traces of Y-type phase ( $\text{Ba}_2\text{Co}_2\text{Fe}_{12}\text{O}_{22}$ ), coexisting with the Z-type.

From the XRD data, the powder appeared to consist of only  $\text{Co}_2\text{Z}$ , a relatively low temperature for single phase  $\text{Co}_2\text{Z}$  to occur, but it was thought unlikely that 100% pure  $\text{Co}_2\text{Z}$  had been formed, as the system is so complex and there are usually either traces of  $\text{Co}_2\text{Y}$  from the formation process<sup>1,4,7,10</sup>.

**Figure 3.** X ray diffraction pattern to the synthesized Z-type hexaferrite at 950 °C.

Due to the sharing of many peak positions the signals of small amounts of these compounds are extremely difficult to distinguish from the major phases in the very convoluted and similar XRD spectra of the hexagonal ferrites. Single phase Z is notoriously hard to produce<sup>1,8</sup>.

Atomic Force Microscopy was used to characterize the powders obtained at 950 °C. It is observed that the particles are uniform in size and shaped as sharply hexagonal plates with nanometric size (Figure 4).

The effect of the partial substitution of Zn and Cu ions on the hysteresis curves for the  $\text{Ba}_3\text{Co}_{1.3}\text{Zn}_{0.3}\text{Cu}_{0.4}\text{Fe}_{24}\text{O}_{41}$  and  $\text{Ba}_3\text{Co}_2\text{Fe}_{24}\text{O}_{41}$  compositions fired at 950 °C is illustrated in Figure 5.

The hysteresis curves measured at room temperature show typical features of magnetically soft ferrites. The saturation magnetization  $M_s$  was obtained by extrapolating the  $M(1/H)$ - curves to  $1/H = 0$ , resulting in the value of 62.34 emu/g for  $\text{Ba}_3\text{Co}_{1.3}\text{Zn}_{0.3}\text{Cu}_{0.4}\text{Fe}_{24}\text{O}_{41}$  and 52.39 emu/g for  $\text{Ba}_3\text{Co}_2\text{Fe}_{24}\text{O}_{41}$ .

The ionic radius of  $\text{Cu}^{2+}$  (0.085 nm) is very close to that of  $\text{Co}^{2+}$  (0.082 nm) and larger than that of  $\text{Fe}^{3+}$  (0.067 nm). The copper ions occupy the octahedral sites in the structure of Z-type hexaferrite and partially substitute cobalt ions<sup>2</sup>. Then, the  $\text{Cu}^{2+}$  distorts the crystalline field due to their electronic configuration, and this behavior results in an increase in  $M_s$  in relation to  $\text{Ba}_3\text{Co}_2\text{Fe}_{24}\text{O}_{41}$ .

Superparamagnetic (SPM) grains of MD particles are difficult to discern, based on the hysteresis properties measured at room temperature, but significant changes in the hysteresis parameters, resulting from a variation in the temperature from 300 K to 4.2 K, can be useful to determine the SPM contribution<sup>1-3</sup>, which can improve the absorbing properties.

Figure 6 shows the temperature effect on the magnetization curves of  $\text{Ba}_3\text{Co}_{1.3}\text{Zn}_{0.3}\text{Cu}_{0.4}\text{Fe}_{24}\text{O}_{41}$  nanopowder, evidencing the magnetic saturation increase with decreasing temperatures.

Using the magnetic hysteresis curves (Figure 6), the magnetic saturation ( $M_s$ ) values attained for the  $\text{Ba}_3\text{Co}_{1.3}\text{Zn}_{0.3}\text{Cu}_{0.4}\text{Fe}_{24}\text{O}_{41}$  hexaferrite nanopowder were obtained, as show in Table 2.

It is known that the magnetic properties of the ferrite affect its microwave absorption. It can be seen that, larger values of  $M_s$  tend to produce larger values of  $\mu$  and, smaller values of  $H_c$  tend to produce high  $\mu$  but with smaller resonant frequencies<sup>12</sup>.

The Langevin's law can be expressed as a function of the magnetic saturation ( $M_s$ ), Boltzman's constant ( $k_B$ ), the magnetic permeability ( $\mu$ ), and the absolute temperature (T), by Equation 1<sup>1</sup>:

$$\frac{M}{M_S} = \coth\left(\frac{\mu H}{k_B T}\right) - \frac{k_B T}{\mu H} \quad (1)$$

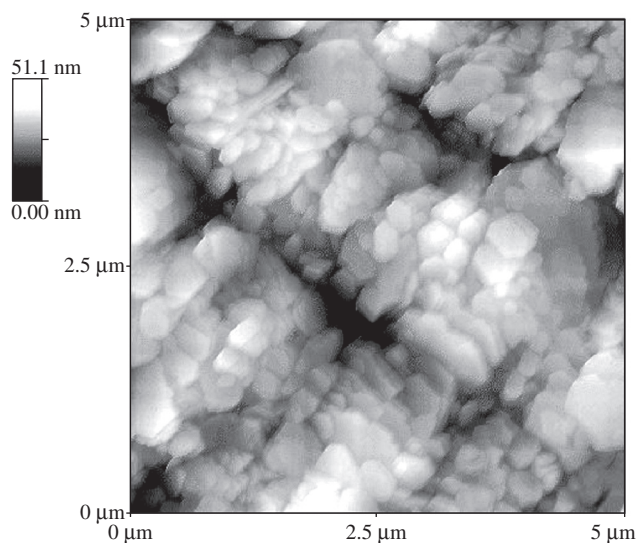


Figure 4. AFM of the  $\text{Ba}_3\text{Co}_{1.3}\text{Zn}_{0.3}\text{Cu}_{0.4}\text{Fe}_{24}\text{O}_{41}$  hexaferrite nanopowder.

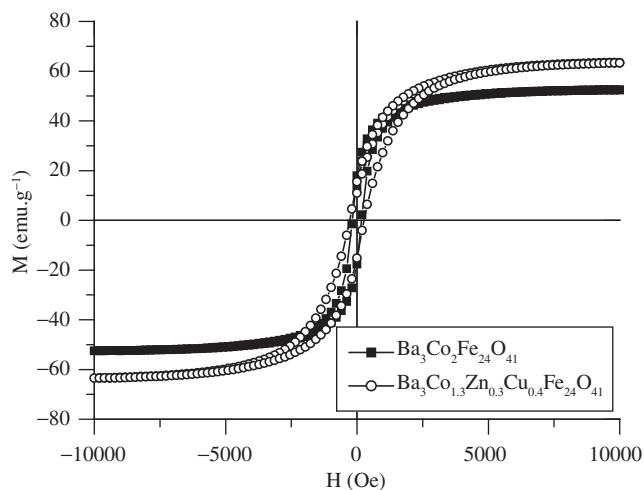


Figure 5. Magnetic hysteresis curves of  $\blacksquare$   $\text{Ba}_3\text{Co}_2\text{Fe}_{24}\text{O}_{41}$  and  $\circ$   $\text{Ba}_3\text{Co}_{1.3}\text{Zn}_{0.3}\text{Cu}_{0.4}\text{Fe}_{24}\text{O}_{41}$  powders.

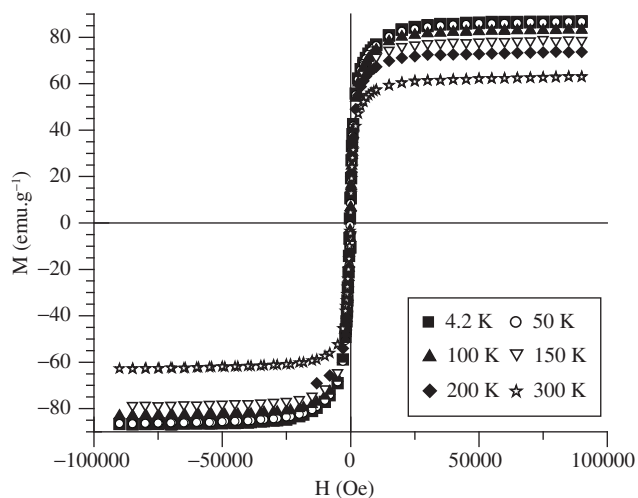


Figure 6. Magnetization curves of the  $\text{Ba}_3\text{Co}_{1.3}\text{Zn}_{0.3}\text{Cu}_{0.4}\text{Fe}_{24}\text{O}_{41}$  hexaferrite at different temperatures (4.2 K to 300 K).

Table 2. Values of magnetic saturation ( $M_s$ ) for the  $\text{Ba}_3\text{Co}_{1.3}\text{Zn}_{0.3}\text{Cu}_{0.4}\text{Fe}_{24}\text{O}_{41}$  nanopowder sample, obtained by the extraction magnetometer (maximum field of 90 kOe).

Temperature (K)	$M_s$ (emu/g)
4.2	87.93
50	87.15
100	83.32
150	78.21
200	74.38
300	63.34

The deviations from the Langevin's law are attributed to interactions between particles, the presence of blocked particles, or relatively high anisotropies<sup>3</sup>.

An ideal superparamagnetic system exhibits a strong characteristic: the magnetization curves ( $M$ ) measured at different temperatures is superposed when plotted on a graph vs.  $H/T$ . However, in practice this behavior is not usually observed owing to several complicating factors such as the presence of magnetic moments' distribution inside a sample, due to the variation of particle sizes<sup>3</sup>.

In nanocrystalline systems the magnetic interactions affect the experimental results. In the case of non-interacting particles, in accordance with the Langevin's law, the  $M/M_s$  vs.  $H/T$  hysteresis curves are expected to superpose, which does not experimentally occur unless perfect superparamagnets are involved<sup>1</sup>.

The system under study ( $\text{Ba}_3\text{Co}_{1.3}\text{Zn}_{0.3}\text{Cu}_{0.4}\text{Fe}_{24}\text{O}_{41}$ ) follows the Langevin's law at temperatures up to 4.2 K, as shown in Figure 7. Hence, there is an expected contribution of typical superparamagnetic behavior.

The normalized hysteresis curve corresponding to the temperature of 4.2 K is not superposable on the others due to the presence of magnetic interactions in the system. The superparamagnetic model itself does not usually explain the macroscopic magnetic behavior in a magnetic nanoparticles' system. This discrepancy can be attributed to the dipolar magnetic interactions that can cause significant alterations in the system's magnetic properties.

The nanometric size of the citrate sol-gel synthesized powder and its SPM contribution can improve in the microwave absorbing properties.

The SEM micrography (Figure 8) for the composition 80:20 (wt. (%)) of the Z-type hexaferrite nanopowder mixed with polychloroprene (CR) used to measuring microwave absorber properties, shows a uniform dispersion in spite of the high weight concentration used (80 wt. (%)) ferrite with (CR) and the tendency of these nanoparticles to form magnetic agglomerates<sup>6</sup>.

It is important, because in the composite ferrites with high weight fractions, ferrite particles can segregate to form magnetic agglomerates and then magnetic poles induced on the surface of the agglomerates will generate the demagnetizing fields, which reduces the effective magnetic moment and the permeability can decrease<sup>6</sup>.

The reflection loss (RL) was calculated by Equation 2, for a given  $f$  (frequency) and  $d$  (thickness) of the absorber:

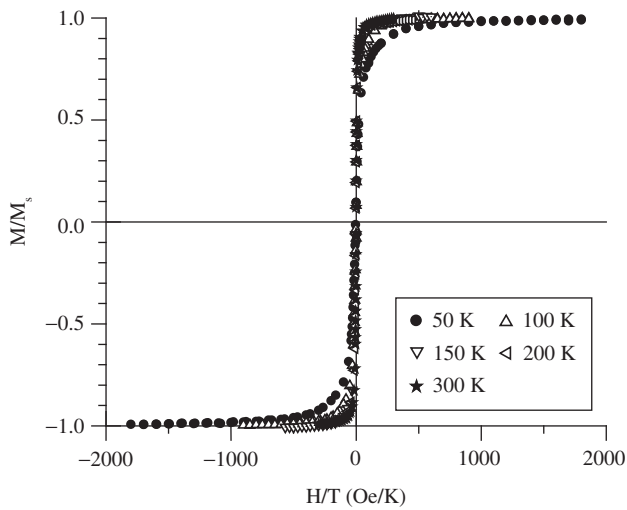
$$\text{RL (dB)} = 20 \log \left| \frac{Z_{\text{in}} - 1}{Z_{\text{in}} + 1} \right| \quad (2)$$

$Z_{\text{in}}$  is the normalized input impedance given by Equation 3:

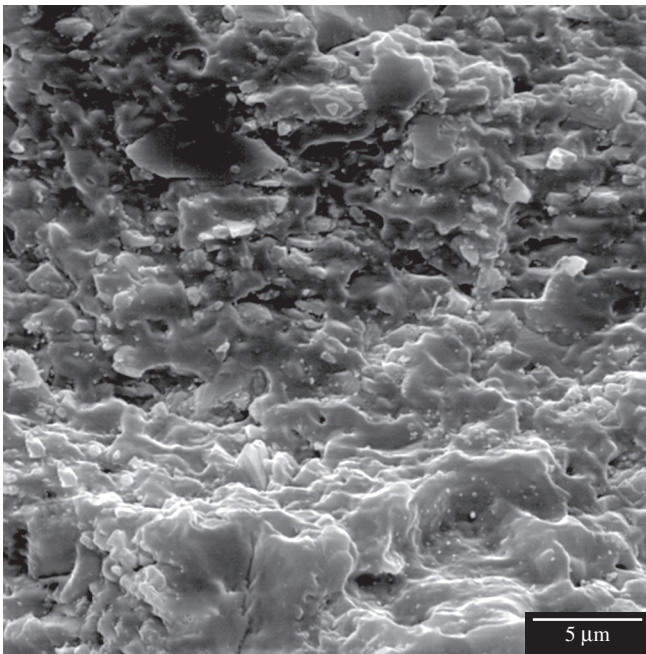
$$Z_{\text{in}} = (\mu/\epsilon)^{1/2} \tanh [j (2 \pi c) (\mu/\epsilon)^{1/2} f d] \quad (3)$$

where  $\mu$  is the complex permeability ( $\mu = \mu' - j \mu''$ ),  $\epsilon$  is the complex permittivity ( $\epsilon = \epsilon' - j \epsilon''$ ) and  $c$  is the velocity of light<sup>2</sup>.

From the result of equation 3, six parameters such as  $\mu'$ ,  $\mu''$ ,  $\epsilon'$ ,  $\epsilon''$ ,  $f$  and  $d$  can determine its absorbing characteristics.



**Figure 7.** Hysteresis cycles normalized by the magnetic saturation ( $M_s$ ) as a function of  $H/T$  for the  $Ba_3Co_{1.3}Zn_{0.3}Cu_{0.4}Fe_{24}O_{41}$  hexaferrite.



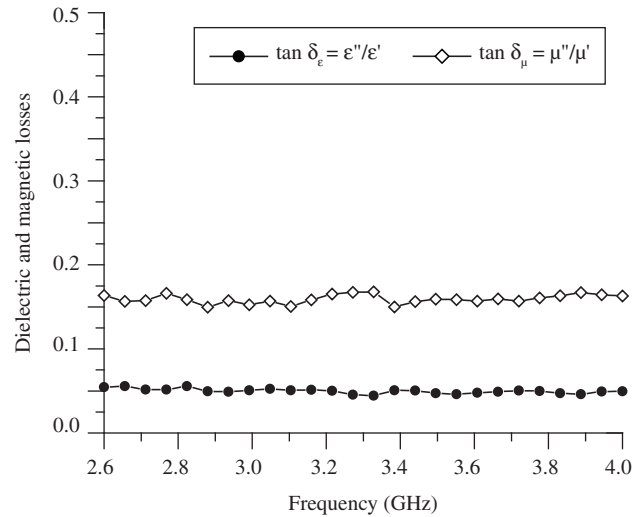
**Figure 8.** Scanning electron micrograph of  $Ba_3Co_{1.3}Zn_{0.3}Cu_{0.4}Fe_{24}O_{41}:CR$  (80:20, wt. (%)) nanocomposite.

Figure 9 and Figure 10 illustrate the frequency dependence of dielectric ( $\epsilon''/\epsilon'$ ) and magnetic losses ( $\mu''/\mu'$ ) for the composite ( $8.00 \times 4.00 \times 0.10 \text{ cm}^3$ ) at the frequency range of 2.6-4.0 GHz and 8.0-16.0 GHz, respectively.

As can be seen, the dielectric losses are very small (about 0.05) and the magnetic losses are higher than the dielectric ones for all frequencies, with higher values for the frequency range 8.0-16.0 GHz.

The change of these losses with frequency may explain the performance of the absorbers, illustrated by the reflectivity curves in Figure 11.

As can be see in Figure 11a, for the S-band (Figure 11a), the best RAM performance at 3.1 GHz was obtained when measuring a thicker sample (6.0 mm).



**Figure 9.** Frequency dependence of dielectric and magnetic losses for the composite at S-band, 1.0 mm thick.

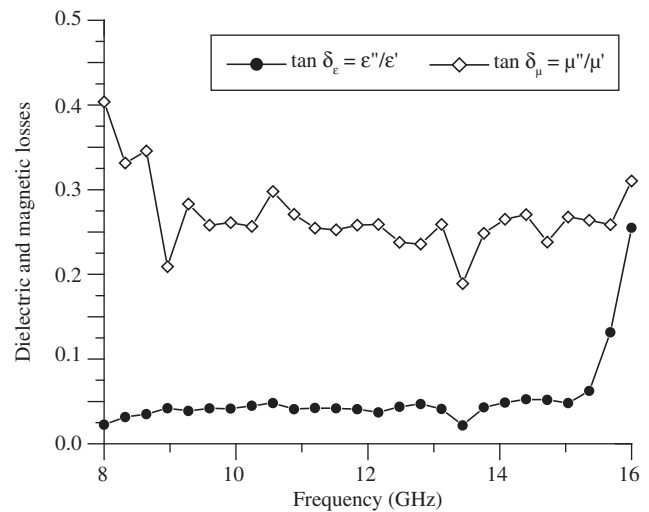


**Figure 10.** Frequency dependence of dielectric and magnetic losses for the composite at X-Ku band, 1.0 mm thick.

From Figure 11b, the substitution of Co by Cu and Zn, resulted in microwave absorptions greater than 90 % at 10.0-12.5 GHz and at 13.0-16.0 GHz, with 2.5 and 2.0 mm thick, respectively.

This behavior may be attributed to the high magnetic loss, caused by the increase of the saturation magnetization of this ceramic that improved the magnetic permeability of the composite.

#### 4. Conclusions

The citrate method promoted the formation of nanocrystalline Z-type hexaferrite at a lower temperature (950 °C) than that employed by the conventional one (1,200-1,300 °C). The introduction of  $Cu^{2+}$  ions improved the magnetic properties of this ceramic illustrated by the increase in the  $M_s$ .

Although the critical size limits for Z-type barium hexaferrite are not yet well defined, the results from the hysteresis curves are representative in the case of nanometric powders.

When the particle size of absorber (ferrite powder) is in nanometric range, the electron can absorb the energy as it leaps from one

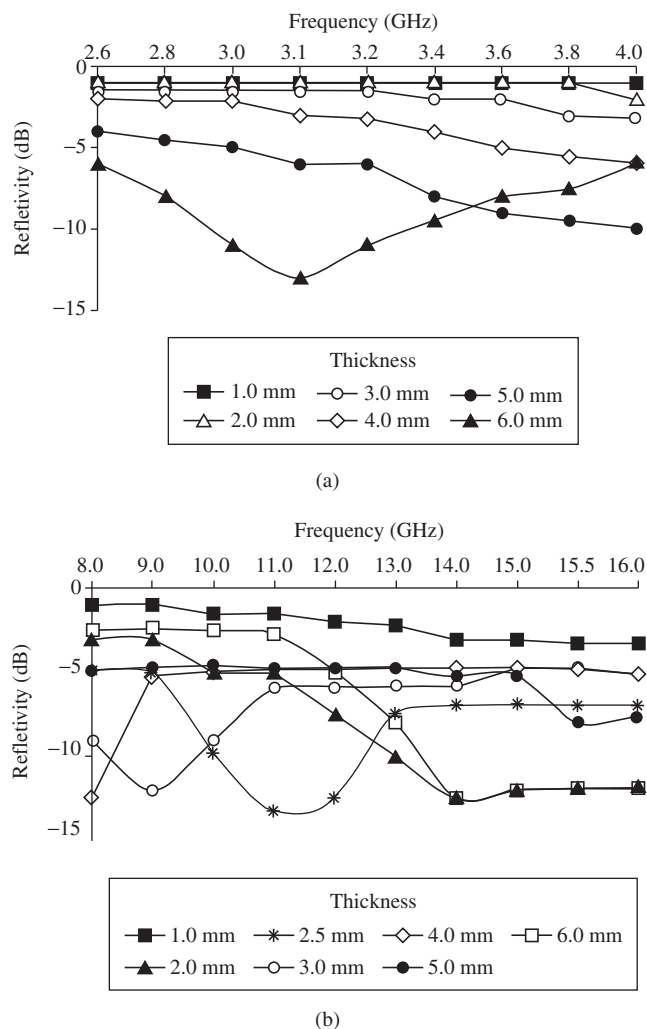


**Figure 11.** Reflectivity curves for 80:20 (wt. (%)) Ba<sub>3</sub>Co<sub>1.3</sub>Zn<sub>0.3</sub>Cu<sub>0.4</sub>Fe<sub>24</sub>O<sub>41</sub>:CR composites for a) S-band and b) X-KU bands.

level to another, which may lead to the increment of attenuation<sup>13</sup>. The quantum size effect in nanocrystalline material makes the electronic energy level split. The spacing between adjacent energy states increases inversely with the volume of the particle<sup>13</sup>.

The partial substitution of Co<sup>2+</sup> for Zn<sup>2+</sup> and Cu<sup>2+</sup> ions resulted in an increase of 9.95 emu/g for the M<sub>s</sub>, and the superparamagnetic contribution improved the magnetic permeability of the ceramics, making possible its application by covering some strategic metallic parts of the Brazilian Frigates' superstructures and so, reducing the radar signature of these targets.

The Ba<sub>3</sub>Co<sub>1.3</sub>Zn<sub>0.3</sub>Cu<sub>0.4</sub>Fe<sub>24</sub>O<sub>41</sub>:CR nanocomposite can be used as a potential magnetic loss material for X/Ku bands, with microwave

absorptions greater than 90% (reflectivity ≤ -10 dB) at 10.0-12.5 GHz and at 13.0-16.0 GHz, with 2.5 and 2.0 mm thickness, respectively. For the S-band, the best RAM performance at 3.1 GHz was obtained when measuring a thicker nanocomposite sample (nanosized ferrite: CR) with 6.0 mm.

## Acknowledgements

The authors gratefully acknowledge the financial support and other forms of aid provided by CNPq, FAPERJ, PEMM/COPPE, CBPF, IF/UFRJ, IPqM and PETROBRAS, which were crucial for the success of this research.

## References

- Ruan S, Xu B, Suo H, Wu F, Xiang S, Zhao M. Microwave Absorptive Behavior of ZnCo-Substituted W-Type Ba Hexaferrite Nanocrystalline Composite Material. *J. Magn. Magn. Mat.* 2000; 212(1-2):175-177.
- Bertorello HR, Bercoff PG, Oliva ML. Model of interactions in nanometric particles of barium hexaferrite. *J. Magn. Magn. Mat.* 2004; 269:122-130.
- Knobel M. Partículas Finas: superparamagnetismo e magnetoresistência gigante. *Rev. Bras. Ens. Fis.* 2000; 22(3):387-395.
- Caffarena VR, Study of the Magnetic and Microwave Absorber Properties of Z-Type Barium Hexaferrite Obtained by Citrate Precursor Method. [Tese de Doutorado]. Rio de Janeiro: Universidade Federal do Rio de Janeiro; 2004.
- Zhang H, Zhou J, Yue Z, Wu P, Gui Z, Li L. Synthesis of Co<sub>2</sub>Z hexagonal ferrite with planar structure by gel self-propagating metho. *Materials Letters* 2000; 43:62-65.
- Nakamura T, Hankui E. Control of high-frequency permeability in polycrystalline (Ba,Co)-Z-type hexagonal ferrite. *J. Magn. Magn. Mat.* 2003; 257:158-164.
- Pinho MS, Gregori ML, Nunes RCR, Soares BG. Performance of Radar Absorbing Materials by Waveguide Measurements for X and Ku-Band Frequencies. *Eur. Pol. Journal* 2002; 38:2321-2327.
- Zhang H, Zhou J, Li L, Yue Z, Gui Z. Dielectric characteristics of novel Z-type planar hexaferrite with Cu modification. *Mater. Lett.* 2002; 55:351-356.
- Kwon HJ, Shin JY, Oh JH. The microwave absorbing and resonance phenomena of Y-type hexagonal ferrite microwave absorbers. *J. Appl. Phys.* 1994; 75(10):6109-6111.
- Queffelec P, Gelin P, Gieraltowski J, Loaec J. A micro strip device for the broad band simultaneous measurement of complex permeability and permittivity. *IEEE Trans. Magn.* 1994; 30(2):224-230.
- Pullar RC. The manufacture and characterization of aligned fibres of the ferroxplana ferrites Co<sub>2</sub>Z, 0,67% CaO-doped Co<sub>2</sub>Z, Co<sub>2</sub>Y and Co<sub>2</sub>W. *J. Magn. Magn. Mat.* 1998; 186:313-325.
- Wallace JL. Broadband Magnetic Microwave Absorbers: Fundamental Limitations. *IEEE Trans. Magn.* 1993; 29:4209-4214.
- Shin JY, Oh JH. The microwave absorbing phenomena of ferrite microwave absorbers. *IEEE Trans. Magn.* 1993; 29(6):3437-3439.